

# A hybrid phosphorus-acid fuel cell system incorporated with oxidative steam reforming of methanol (OSRM) reformer



Cheng-Ping Chang<sup>a</sup>, Yen-Chih Wu<sup>a</sup>, Wei-Yen Chen<sup>a</sup>, Chin Pan<sup>a</sup>, Yu-Chuan Su<sup>a</sup>,  
Yuh-Jeen Huang<sup>b,\*,\*\*</sup>, Fan-Gang Tseng<sup>a,c,\*</sup>

<sup>a</sup> Department of Engineering and System Science, Frontier Research Center on Fundamental and Applied Sciences of Matters, National Tsing Hua University, Taiwan

<sup>b</sup> Department of Biomedical Engineering and Environmental Sciences, National Tsing Hua University, Taiwan

<sup>c</sup> Research Center for Applied Sciences, Academia Sinica, Taiwan

## ARTICLE INFO

### Article history:

Received 4 July 2018

Received in revised form

30 October 2019

Accepted 28 January 2020

Available online 12 February 2020

### Keywords:

OSRM reformer

PAFC

Reformed methanol fuel cell

Integrated reformer with fuel cell

## ABSTRACT

In this paper, a phosphoric acid fuel cell integrated with reformer and evaporator is demonstrated. Oxidative steam reforming of methanol (OSRM) process is employed in this system in cooperated with a high efficient evaporator, and the reacted gas is sent into a phosphorus-acid fuel cell (PAFC) for direct power generation after surplus methanol/water filtration. The results show that the maximum power density of this hybrid system achieves 277 mW/cm<sup>2</sup> without CO<sub>2</sub> removal, while it achieves 485 mW/cm<sup>2</sup> when employing pure hydrogen as the fuel.

© 2020 Elsevier Ltd. All rights reserved.

## 1. Introduction

In the past decades, proton exchange membrane fuel cell (PEMFC) has been a common topic in the development of fuel cells. For the well-developed PEMFC using Nafion® from DuPont as electrolyte, the polymer membrane will lose moisture when operating above 90 °C, further severely degrades the fuel cell performance [1]. At such operating temperature, platinum catalysts on the electrodes of the fuel cell can be easily poisoned by impurities, such as carbon monoxide (CO), in the product of reformed alcohols, natural gas or gasoline [2].

Compared to low temperature PEMFC, High-temperature PEMFC (HT-PEMFC), such as phosphoric acid fuel cell (PAFC), shows decent performance between 120 and 200 °C without the aforementioned issues. According to past studies, HT-PEMFCs can tolerate CO at a content of 1–3% [3–6] (compared with 20 ppm for

PEMFC operating below 100 °C), which makes it an appropriate electricity generating device for the integration with reformer. Among the hydrogen-rich compounds, methanol is most widely used hydrogen source due to its high hydrogen/carbon ratio, high energy density (2500WhL<sup>-1</sup> for hydrogen and 5000WhL<sup>-1</sup> for liquid methanol [7]), cost-effective, low evaporating-temperature, and relatively low reforming temperature. Comparing with direct methanol fuel cell (DMFC), reformed methanol fuel cell (RMFC) possesses higher performance on power due to the slower anodic half-reaction for methanol oxidation and methanol crossover in DMFCs [8–10]. The introduction of the methanol reformer makes fuel cells much more portable and simplify the refueling process instead of using compressed hydrogen as the fuel source. Therefore, HT-PEMFC is a practical choice for RMFC system. In HT-PEMFCs, polybenzimidazole (PBI) ion-exchange membrane doped with phosphoric acid was widely used [9,11–14] and operated well at the temperature interval between 100 and 200 °C. Higher temperature may lead to degradation due to phosphoric acid (H<sub>3</sub>PO<sub>4</sub>) leaking, dehydration of H<sub>3</sub>PO<sub>4</sub>, and Pt catalyst agglomeration etc. [15–17].

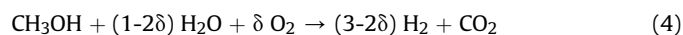
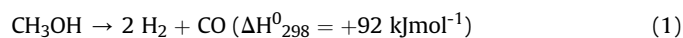
In regarding methanol reforming processes, hydrogen can be produced via various reforming reactions, such as thermal decomposition of methanol (DM), partial oxidation of methanol (POM), steam reforming of methanol (SRM), or oxidative steam

\* Corresponding author. Department of Engineering and System Science, Frontier Research Center on Fundamental and Applied Sciences of Matters, National Tsing Hua University, Taiwan.

\*\* Corresponding author.

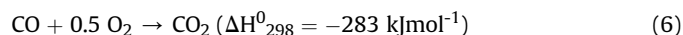
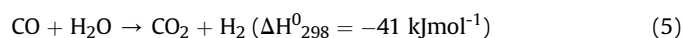
E-mail addresses: [yjhuang@mx.nthu.edu.tw](mailto:yjhuang@mx.nthu.edu.tw) (Y.-J. Huang), [fangang@ess.nthu.edu.tw](mailto:fangang@ess.nthu.edu.tw), [fangangtseng@gmail.com](mailto:fangangtseng@gmail.com) (F.-G. Tseng).

reforming of methanol (OSRM). The equations of these reactions are as followed (Eqs(1)–(4)) [18], respectively:

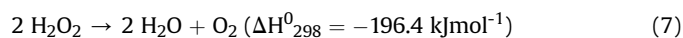


Among them, DM reaction is usually not considered to integrate with fuel cells due to its sluggish reacting rate and high CO content in the product [19]. POM reaction is an exothermal-reaction and works at a relatively low temperature (180–250 °C, compared to 240–350 °C for SRM), theoretically allowing to sustain its operating temperature and possessed with quick start-up [20–24]. However, its hydrogen producing rate is 33% lower than SRM reaction. Other difficulties such as hot spot caused by the acute heat released during the reaction and the provision of the gas reactant (oxygen) pose complexity for real applications.

So far, SRM has been the mostly considered way to produce hydrogen for fuel cells due to its high hydrogen yield and simple reactants supply (methanol and water, liquid only). However, SRM is an endothermal reaction requiring external heat supply [25,26]. On the other hand, reforming reactions tend to have higher CO yield at higher operating temperature [27]. Therefore, a water-gas shift (WGS) reactor or a preferential oxidation (PROX) reactor is often equipped to remove CO. The equations are as followed (Eqs (5) and (6)) [28–31].



On the other hand, OSRM reaction, also known as autothermal reforming (ATR) of methanol, is a combination of POM and SRM. The enthalpy of the reaction is decided by the percentages of the two reforming reactions. In Eq (4),  $\delta$  is the coefficient that represents the ratio of  $\text{O}_2/\text{MeOH}$ , the coefficient  $\delta$  lies between 0 and 0.5. The reaction can be heat equilibrium by deliberate arrangements ( $\delta=0.125$ ) [23,32], which means the reaction can sustain at its operating temperature by well heat insulation without external heat supply. Therefore, OSRM is applied in this study for the integrated HT-PEMFC. In order to simplify the fuel cell system, hydrogen peroxide ( $\text{H}_2\text{O}_2$ ) is substituted for oxygen and water appropriately. Hydrogen peroxide is a colorless liquid, slightly more viscous than water. Due to hydrogen peroxide is thermodynamically unstable, it self-decomposes completely into water and oxygen at 150 °C (Eq (7)). Thus hydrogen peroxide was mixed with methanol to be the reactants of OSRM reaction in the current study. The  $\text{H}_2\text{O}_2$ -OSRM system facilitates the design of the fuel cell system [33].



To get high conversion rate of OSRM reaction, CuPdCeZn is chosen as the catalyst for this experiment. CuZn is a common catalyst used in methanol reforming reaction. The addition of Ce can reduce the production of CO effectively because of its extra oxygen vacancies [34]. While Palladium is an effective decomposition catalyst, which help on the formation of hydrogen and carbon monoxide from methanol. However, when Pd is prepared with Zn, the selectivity will shift to  $\text{CO}_2$  [35]. In addition, adding Pd and Ce can also increase Cu dispersion and reduce particle size [36].

Beside catalyst, design of flow channels also affects the performance of reaction. Several researches about the flow channel design of methanol reformers were reported, including multi-channel micro packed-bed reactor, cross-U type reactor, etc. [37–39]. In this paper, we employed a Swiss-rolle shape flow channel to enhance the thermal efficiency of OSRM reformers. The reaction starts from the center of the flow channel, in which the POM reaction occurs rapidly. The shape can help the excess heat from the center spread out to the surrounding of the channels, where the relatively slow reaction, SRM, can be supported. By the arrangement of various concentrations of catalyst along the spiral channels, POM and SRM reactions can be better manipulated. By accurate arrangement, the overall reaction can reach a heat balance and the partial high temperature situation can be much avoided.

To further increase the operation efficiency of reformers, recent researches also included evaporator before reformer [40] to completely evaporate liquid fuel into an even mixture of gas/vapor. When the fluid passes through the evaporator, the fluid can be effectively heated in advance to completely vaporize the fluid to prevent the incompletely vaporized fluid from entering the reformer, thereby improving the methanol conversion rate of the reformer. There's also studies incorporated miniature evaporators, with pin fin heat sinks set at the corners [41], to increase the heat transfer effect. However, most of the flow channel areas in those designs did not consider cooling fins, as a result, the thermal efficiency of the evaporator would not be high (usually less than 33% [42]). In this study, a micro evaporator is employed by using heat sinks with straight-shaped channel design [43] to enhance the heat transfer, thus the thermal efficiency can approach 63.3%.

When considering the integration of reformers with fuel cell systems, several studies described the configurations, however, most of them employed SRM reactions. C. Pan et al. [3] first introduced a direct-thermal-contact HT-PEMFC stack with a SRM reactor. At 260 °C, hydrogen yield achieved ~4200 mL/min by 149 g catalyst while only ~1200 mL/min is produced at 200 °C. For the integrated system test, the PBI-based HT-PEMFC shows a severe drop comparing with hydrogen as fuel. The generated power reached 344 mW/cm<sup>2</sup>. F. Weng et al. [44] introduced a two-stage reforming system integrated with PBI-based HT-PEMFC. The first reformer is combined with a catalytic methanol combustor operating at 240 °C. Afterwards, the second reformer is combined with the HT-PEMFC operating at 200 °C. As a result, two-stage reformer has a more stable product flow rate which responses to stable fuel cell operation and the power generation reached 250 mW/cm<sup>2</sup>. Yet these devices were merely arranged physical contact of fuel cells and reformers by using holders or a cover without fully integration. G. Avgouropoulos et al. [45–48] introduced an internal methanol reforming fuel cell system. The reforming catalyst is composed of copper foam, acting as the current collector simultaneously, attached to the anodic side of membrane-electrode-assembly (MEA). However, the corrosion caused by the leaked phosphoric acid results in severe degradation of the reformer. Therefore, a bipolar plate with serpentine channel is installed to improve the stability. In recent studies, P. Reberinha et al. [49,50] introduced a bipolar plate with serpentine channels on the both sides. The inner side naturally contact with the MEA; while the outer side is filled with reforming catalyst, sealed with a silicon gasket. The integrated fuel cell test shows a nearly overlapped polarization curve for reformed gases and pure hydrogen as fuel between 180 and 200 °C. Furthermore, power density achieved 330 mW/cm<sup>2</sup> with reformed gasses and air supply at 180 °C [50].

In our past studies, H.-S. Wang et al. [51], in addition to the integrated systems operated with SRM reactions mentioned above, introduced an integrated system equipped with a micro-POM-reformer and a home-made HT-PEMFC based on  $\text{H}_3\text{PO}_4$  doped

glass micro fiber/polytetrafluoroethylene (GMF/PTFE) composite membrane (the same MEA is used in this study). Through the fill-and-dry process and the centrifugal process, the silicon-based microfluidic channels enhance the surface area of the catalyst, which results in high hydrogen yield (per catalyst weight) at relatively lower temperature at 180 °C [52]. The composite membrane possesses the two materials' advantages. The inner GMF with micro-pores absorbs plenty of electrolyte to gain high proton conductivity; meanwhile, the outer PTFE films with nano-pores prevent  $H_3PO_4$  from leaking [53]. Power density achieved 132  $mW/cm^2$  with reformed gases and oxygen for the integrated system. However, the total hydrogen producing rate and power density is limited due to the spatial limitation of the micro-channel. Therefore, in order to enhance the hydrogen yield and power density, we enlarge the methanol reformer and added an evaporator to enhance the hydrogen producing rate to provide enough hydrogen atom for the fuel cell. And the power density has been increased into 277  $mW/cm^2$  in the current research by the integrated with the aforementioned components.

## 2. Experimentals

The overall schematic of the hybrid OSRM reformer and PAFC system and its operation process are shown in Fig. 1. Mixture of methanol and hydrogen peroxide, served as the fuel, is sent to a micro evaporator by a tubing pump. Through micro evaporator, the mixture evaporates rapidly into gas phase. Under 140 °C, hydrogen peroxide is fully decomposed into oxygen and water. The mixture is reformed into hydrogen and carbon dioxide by OSRM reaction in the reformer. The residual methanol and water is removed by ice bath. PAFC starts working after anode and cathode is filled with reformed gases and pure oxygen, respectively.

The design and operation principle of each component are described in the following sections.

### 2.1. Micro-evaporator

In this experiment, the integrated RMFC system is configured as shown in Fig. 1. The chip is placed in a thermal insulation fixture and use a peristaltic pump at the inlet to introduce the mixture of methanol and hydrogen peroxide (4:1) into the channel. In the rear 1/3 area of the evaporator [54], heating power is provided by using a heater. The outlet temperature and the copper wall temperature above the heater is measured by T-type thermocouples connected to a data acquisition device for calculating the thermal efficiency (see Fig. 2). The whole device is schematically shown as Fig. 3(a).

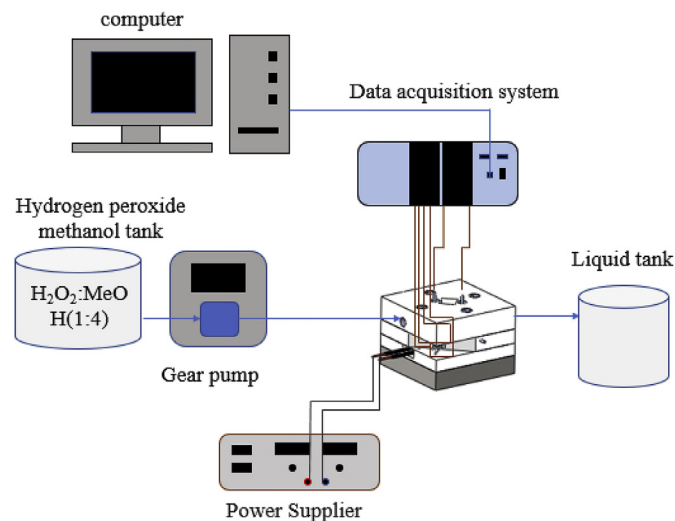


Fig. 2. Thermal efficiency test system for evaporator.

The micro-channel evaporator used in this experiment is a strip-shaped fin structure. The evaporator consists of 52 straight runners with a length of 10.8 mm, width of 0.15 mm, and height of 0.1 mm. The result will be compared with the flow channel with empty-chamber evaporator in the later session. The evaporator is made of silicon by photolithography and deep silicon dry etching processes to obtain the flow channel structures as shown in Fig. 3(b), and the channels are enclosed by a pyrex glass plate through anodic bonding process.

### 2.2. OSRM reactor

The catalyst used in the OSRM reactor is a copper-based catalyst, CuPd/CeZnO, prepared by co-precipitation of metal nitrates in aqueous solution. After filtering and washing, the precipitate is dried overnight and calcined in air. The catalyst particle is crushed and sieved to 60–80 mesh for the preparation of reaction.

The reformer is designed with a swiss-roll flow channel as shown in Fig. 4(a), and made of aluminum for light weight and high heat conductivity. The rectangle area beside the flow channel is set as a heating area. A battery-charge electrical heater is installed on the area. The heater raises the temperature from room temperature to the reaction temperature. And a heat-resistant gasket is put between the flow channel and the cover to avoid gas leakage. The

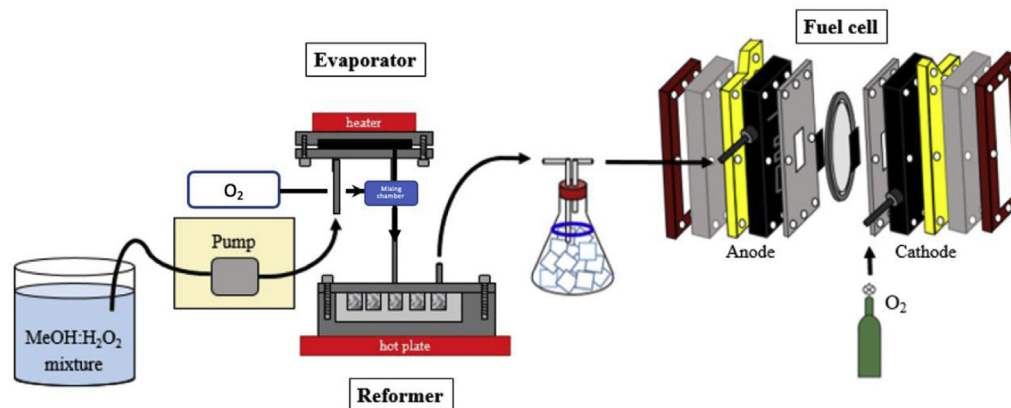


Fig. 1. The schematic illustration of the integrated RMFC system.

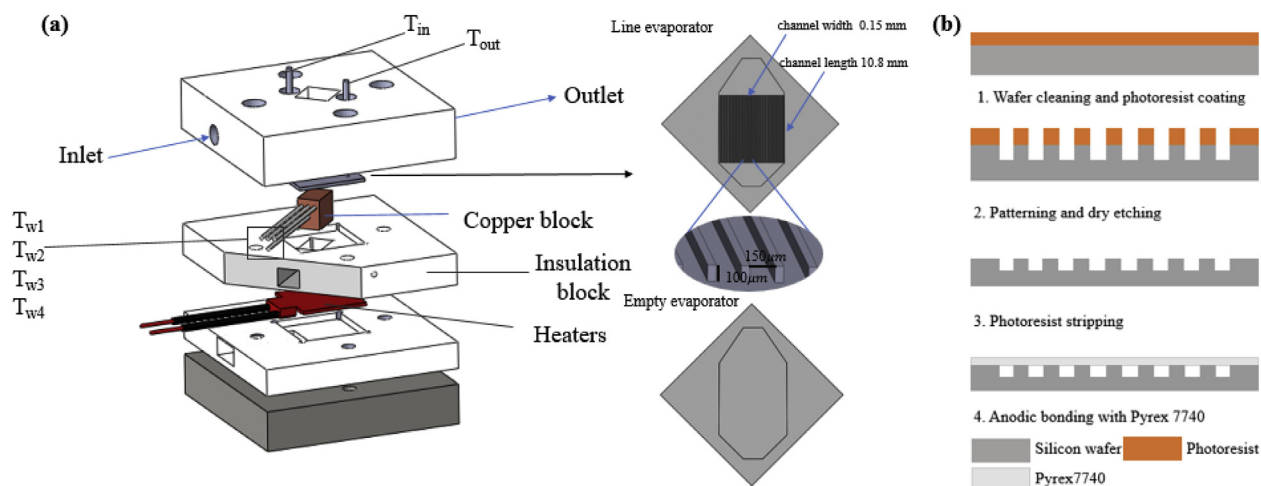


Fig. 3. (a) The design schematic of evaporator and (b) the fabrication process of evaporator.

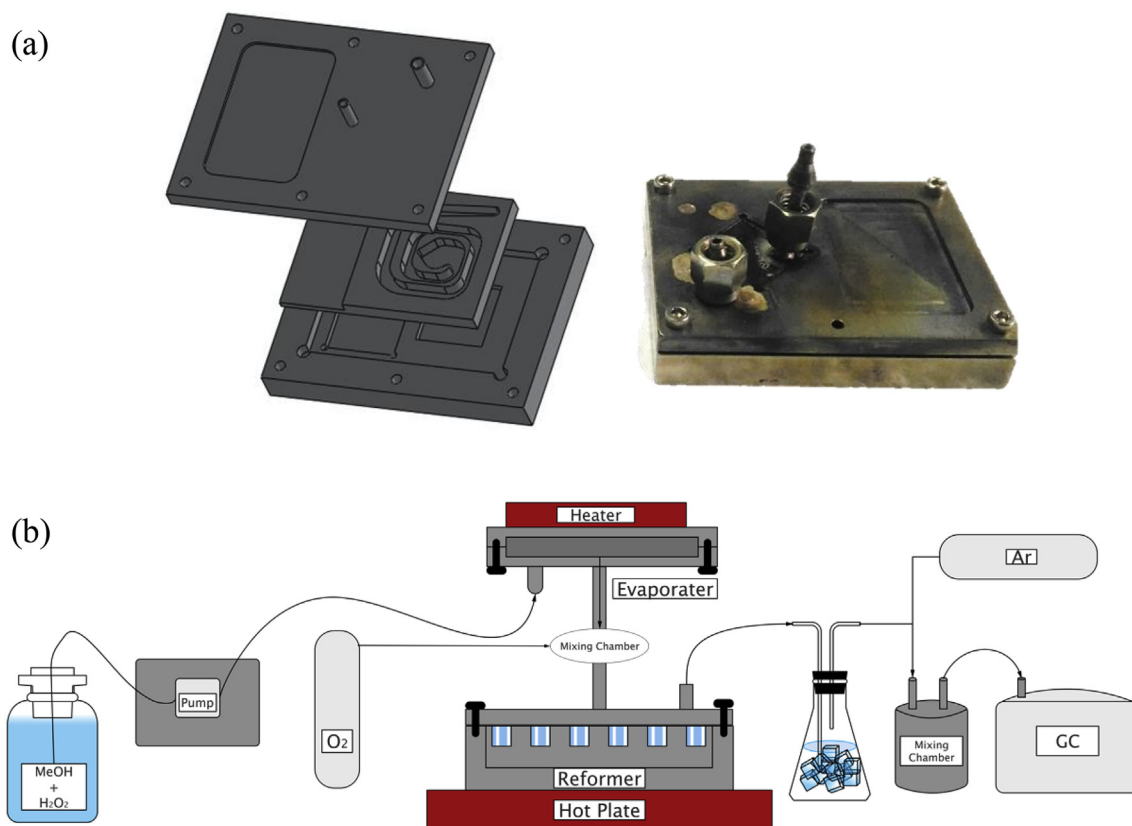


Fig. 4. (a) Design schematic and image of Swiss-roll reformer. (b) Test system for OSRM reformer and a micro evaporator.

whole reaction area is covered by stainless steel. The flow rate, conversion rate and the CO concentration were measured by the Gas Chromatography (GC) system as shown in Fig. 4(b).

### 2.3. Preparation of PAFC

The preparation of the MEA of PAFC is described in our past study [53]. 20% Pt/Vulcan XC-72 carbon (from Premetek) was dispersed in distilled water, isopropyl alcohol. 35% PTFE solution is added to the catalyst ink. After supersonic shocking for dispersing the catalyst uniformly, catalyst ink was sprayed (via nitrogen) on

carbon clothes (EC-CC1-060 T, from ElectroChem) which was heated to evaporate solvent. After the platinum loading achieved  $1 \text{ mg/cm}^2$ , and the samples were then left in oven for sintering at  $340 \text{ }^\circ\text{C}$  for 15 min to evaporate solvent totally and melt PTFE for better catalyst binding.

Before assembly GMF (GF/B, from Whatman) and PTFE film (from Fulli-Jolli) together, PTFE hydrophilic treatment was carried out by soaking in methanol under ultrasonic agitation for 15 min to allow  $\text{H}_3\text{PO}_4$  fully absorbed by the nano-pores of PTFE film. GMF and methanol treated PTFE (mPTFE) were fully loaded with electrolyte by soaking in  $150 \text{ }^\circ\text{C}$   $\text{H}_3\text{PO}_4$  and ambient temperature  $\text{H}_3\text{PO}_4$

for 15 min, respectively. The two films were brought together carefully from one side to the other to form a three-layer composite membrane, as the schematic shown in Fig. 5. The active area of the MEA is  $1\text{ cm} \times 1\text{ cm}$ .

#### 2.4. Test of hybrid reformer and PAFC system

The integrated system includes a micro-evaporator, OSRM reformer, and PAFC, as shown in Fig. 1 Through a tubing pump, MeOH and 50w.t.%  $\text{H}_2\text{O}_2$  mixture (volumetric ratio = 3:1) is fed at a volumetric rate of 0.16 sccm into the evaporator which operates at  $150\text{ }^\circ\text{C}$ . Then the MeOH vapor and decomposed  $\text{H}_2\text{O}_2$  (converted molar ratio  $\text{MeOH}:\text{H}_2\text{O}:\text{O}_2 = 1:0.68:0.12$ ) is transferred to the reformer which is heated by a hot plate. The reformer is maintained at  $230\text{ }^\circ\text{C}$ , measured by a thermal couple. The residual methanol in the reformat is then condensed in a cold water bath. Finally, the hydrogen-rich products flow into the anode of the fuel cell. To show the difference of the performance using reformat gases or pure hydrogen as the fuel, 100 sccm pure hydrogen is fed to examine the effect of the usage of reformat. For the oxidant at the cathode, pure  $\text{O}_2$ -feeding is kept at 100 sccm during the entire testing. Voltages from 1.0 V to 0.1 V is measured in steps of 0.05 V and 8 s by a customized fuel cell test station (Mini50, Hephas, USA). Fig. 8 is the illustration of the whole system.

### 3. Results

#### 3.1. Thermal transfer and efficiency of the micro-evaporator

Compared with the empty evaporator, the additional fins of line evaporator can effectively increase the critical heat flux and delay the channel dry-out phenomenon. The different behavior between empty evaporator and line evaporator are shown in Fig. 6. The heat dissipation fins enable the line evaporator with higher critical heat fluxes than the empty evaporator. The main reason is that the fins can limit the size of the bubble and the growth of the dry zone

(Fig. 7), which would radically decrease the thermal removal ability. So it comes to the result the line structure design can reach higher critical heat flux.

The thermal efficiency testing results of the evaporators are shown in Fig. 8, illustrating the comparison of empty chamber type and line type evaporators at a heating temperature up to  $250\text{ }^\circ\text{C}$ . The line type evaporator can provide a much better heat exchange efficiency than that of the empty chamber one. The highest efficiency of 63.3% at a heating power of 11 W is also reached by the line type evaporator.

#### 3.2. Reformatted gases from OSRM reformer

The measurement results of the outlet gases of the reformer is shown in Fig. 9(a), depicting that  $230\text{--}250\text{ }^\circ\text{C}$  is an appropriate operation temperature where the conversion rate of the reformer is relatively high of 70–90% while the CO concentration is still kept at a low value of 0.5%, suitable for PAFC operation. The figure shows there still remain some methanol and may cause a decrease to the open circuit voltage (OCV) of fuel cell. As a result, a cold water bath is employed to remove most of the residual methanol and water from the reformat gas. The compositions of the reformatted gases are shown in Fig. 7(b), showing a roughly 25% and 75% of  $\text{CO}_2$  and  $\text{H}_2$ , respectively, generated between 230 and  $250\text{ }^\circ\text{C}$ .

#### 3.3. Testing of the integrated system

Before comparison, the performance of PAFC was tested by introducing pure hydrogen as the fuel and operated from  $90\text{ }^\circ\text{C}$  to  $140\text{ }^\circ\text{C}$ , as the results shown in Fig. 10. The maximum power density achieved  $485\text{ mW}/\text{cm}^2$  at  $140\text{ }^\circ\text{C}$ . However, the composite membrane degrades severely above  $150\text{ }^\circ\text{C}$  mainly due to the loss of hydrophilicity of PTFE [53]. Therefore, the testing condition for the integration is chosen at  $140\text{ }^\circ\text{C}$  for the testing of the integrated reformer-PAFC system. And Fig. S1 shows the composite membrane is capable to operate stably for 10 h after a initial settlement.

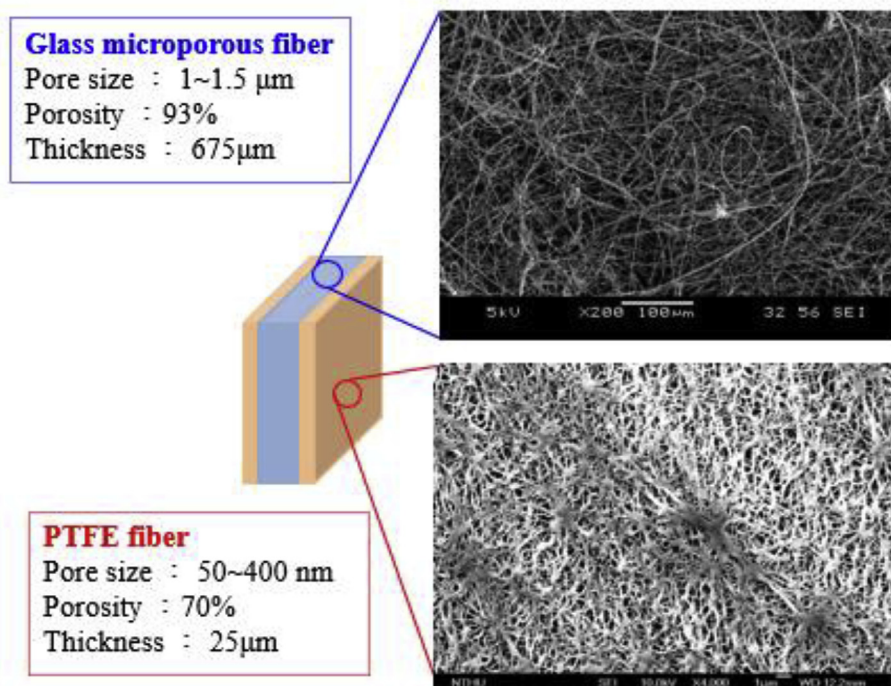


Fig. 5. The schematic picture and SEM image of GMF/PTFE composite membrane.

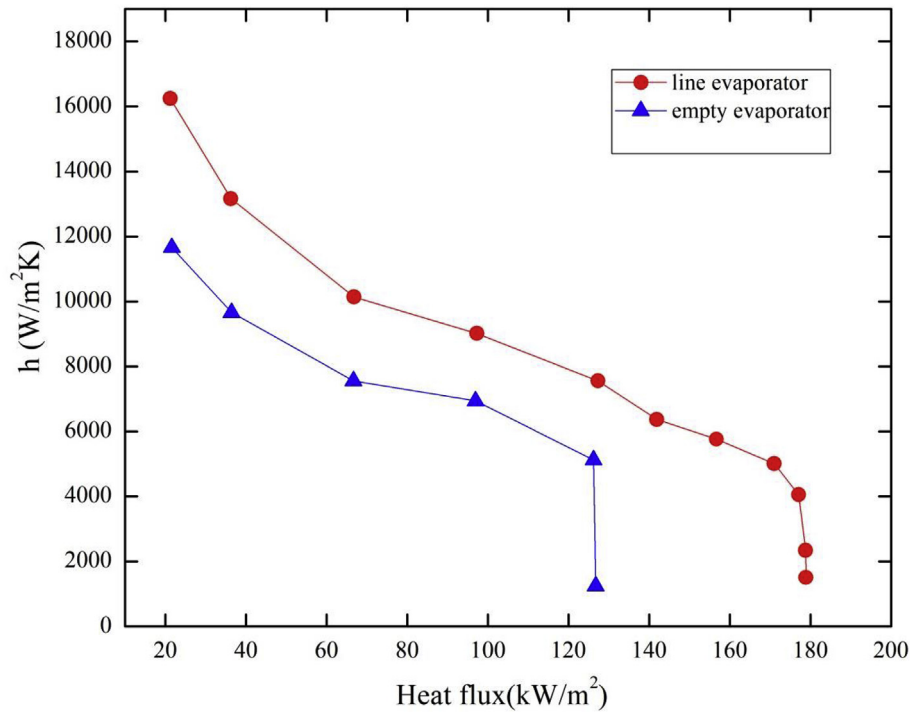


Fig. 6. Heat transfer coefficient for different evaporators as a function of effective heat flux.

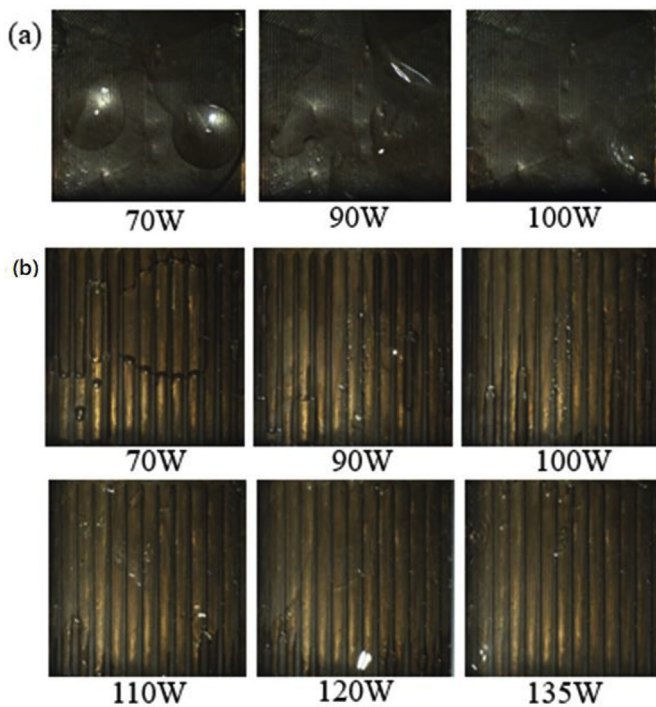


Fig. 7. Visual test of line evaporator and empty evaporator.

The testing result of the integrated reformate fuel cell system is shown in Fig. 11. The OCV of the reformate fuel cell system remained the same as hydrogen fuel cell system, showing little crossover of fuel and little methanol remained for the successful removal of residual methanol and water. The peak power density of the reformate fuel cell illustrated 277  $\text{mw}/\text{cm}^2$ , which was a 43% reduction of that by the pure hydrogen fuel cell system at

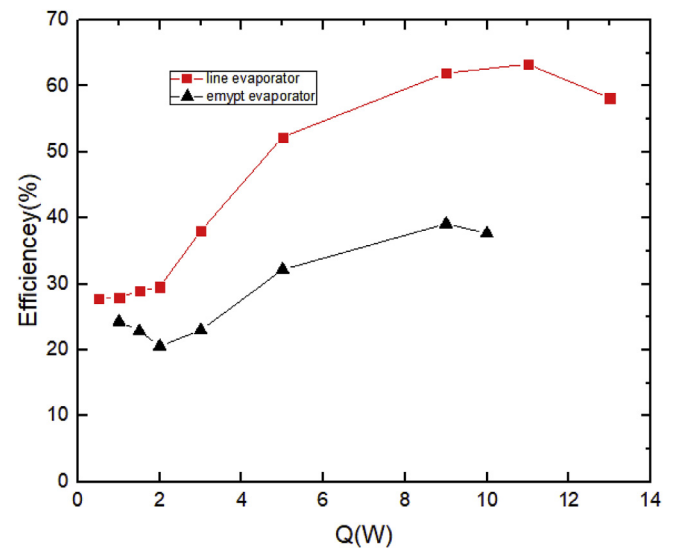


Fig. 8. Thermal efficiency of evaporators.

the same operation temperature of 140 °C. This reduction may partially attribute to the impurity of the reformatted gases containing more than 25%  $\text{CO}_2$  and small amount of CO. It also cause severe mass transport problem at high current density. Increasing the operation temperature of the fuel cell may enhance the CO resistance of electrode, however, it may degrade the performance of the current fuel cell. An alternative way is adding a water gas shift (WGS) reaction channel to not only reduce the concentration of CO but also increase the amount of hydrogen, which will be considered to implement in the future. Long-term test is performed and the result is shown in Fig. S2. It is less stable when compared to the pure hydrogen one because of the remaining CO and other minor gases, which can be further

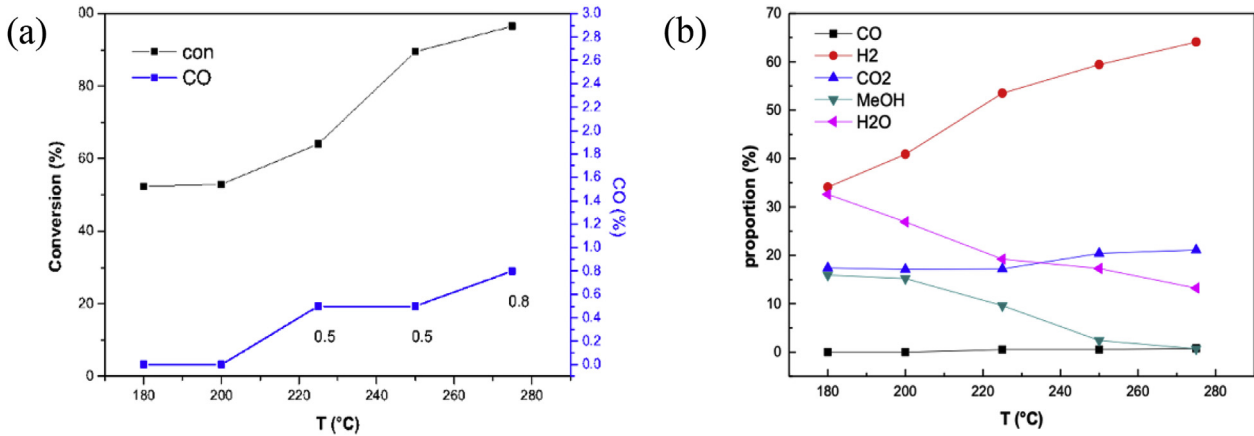


Fig. 9. (a) Conversion rate of OSRM reactor (b) Composition of the reformat gas.

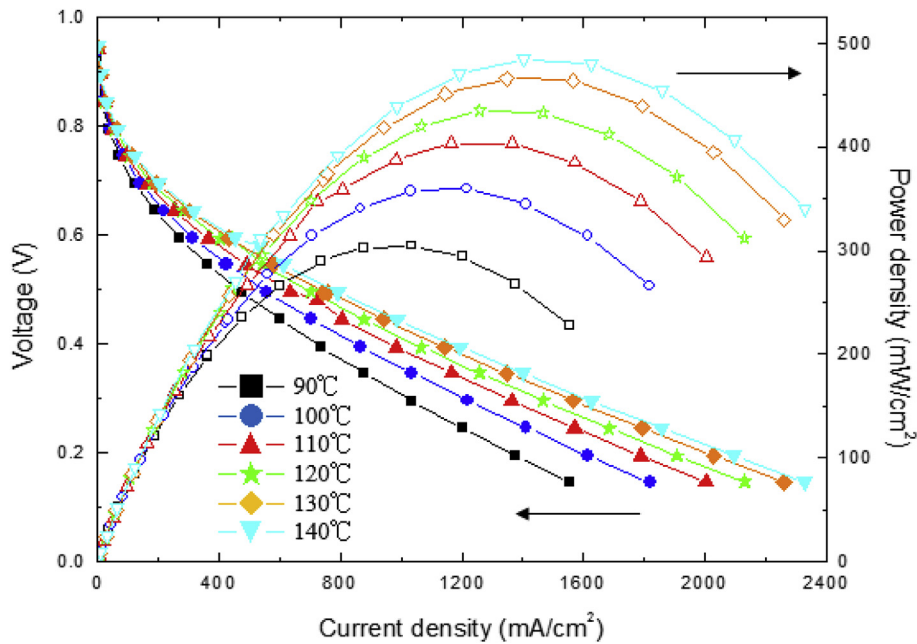


Fig. 10. Polarization curves and power density of the GMF/PTFE composite membrane operating between 90 °C and 140 °C in a step of 10 °C. 100scm hydrogen and 100scm oxygen is supplied at the anode and cathode respectively.

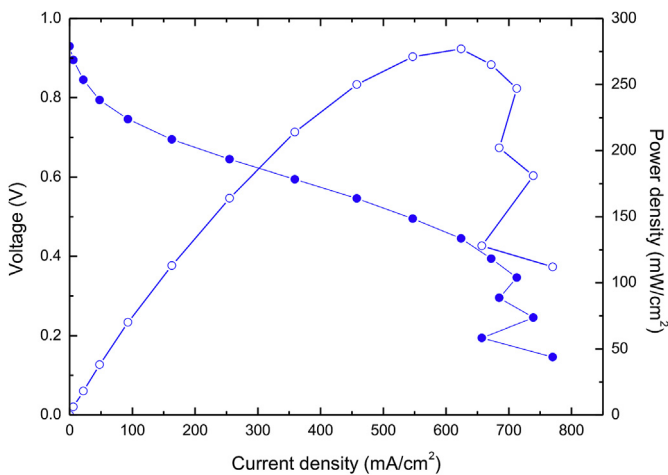


Fig. 11. Polarization curves and power density of the reformat fuel cell system.

improved by removing those impurity before the introduction into the fuel cell.

The performance of the integrated system when compared to the other studies, including One-stage and two-stage SRM system by F. Weng et al. [44], low-temperature POM system by H.-S. Wang et al. [55], and a heat exchange SRM system by G. Schuller et al. [56], are illustrated in Table 1. It seems the current system can offer higher peak power density (277 mW/cm<sup>2</sup>) and more hydrogen production density (485 mW/cm<sup>2</sup>) than others with a higher hydrogen generation rate at a lower temperature (140 °C).

#### 4. Conclusion

In this research, a hybrid reformat fuel cell system, which integrates an oxidative steam reforming of methanol (OSRM) reformer, a micro evaporator, and a phosphorus-acid fuel cell (PAFC), is introduced for direct power generation after surplus methanol/water filtration. The power density of the integrated

**Table 1**  
Comparison of different integrate system.

	Reformer	Fuel Rate (sccm)	FC T (°C)	MR T (°C)	Peak Power (mW/cm <sup>2</sup> )	Hydrogen (mW/cm <sup>2</sup> )
This Study	OSRM	0.16	140	230	277	485
F. Weng	One-Stage	0.25	200	200	200	344
	Two-Stage	0.42	200	240/200	250	344
H.-S. Wang	LTPOM	45 <sup>a</sup>	140	180	132	288
G. Schuller	SRM	–	180	250	216	–

Note. FC T = Fuel Cell Temperature; MR T = Methanol Reformer Temperature. <sup>a</sup>Reformed Gas Flow Rate.

system has achieved 277 mW/cm<sup>2</sup> under a operation condition at 140 °C for fuel cell and 230 °C for the methanol reformer with a feeding rate of fuel at 0.16 sccm, which would be suitable for the application of direct power generation.

### Declaration of competing interest

The authors declare that they have no known competing financial interests or personal relationships that could have appeared to influence the work reported in this paper.

### Acknowledgement

The research was financially supported by Ministry of Science and Technology (MOST) of Taiwan (MOST 105-3113-E-007-002-).

### Appendix A. Supplementary data

Supplementary data to this article can be found online at <https://doi.org/10.1016/j.renene.2020.01.137>.

### References

- [1] P. Choi, N.H. Jalani, R. Datta, Thermodynamics and proton transport in nafion, *J. Electrochem. Soc.* 152 (2005) 123–130.
- [2] J. Larminie, A. Dicks, M.S. McDonald, *Fuel Cell Systems Explained*, vol. 2, J. Wiley Chichester, 2003, pp. 207–225.
- [3] C. Pan, et al., Integration of high temperature PEM fuel cells with a methanol reformer, *J. Power Sources* 145 (2005) 392–398.
- [4] S. Søndergaard, L.N. Cleemann, J.O. Jensen, N.J. Bjerrum, Influence of carbon monoxide on the cathode in high-temperature polymer electrolyte membrane fuel cells, *Int. J. Hydrogen Energy* 42 (2017) 3309–3315.
- [5] S.K. Das, A. Reis, K.J. Berry, Experimental evaluation of CO poisoning on the performance of a high temperature proton exchange membrane fuel cell, *J. Power Sources* 193 (2009) 691–698.
- [6] M. Boaventura, I. Alves, P. Ribeirinha, A. Mendes, The influence of impurities in high temperature polymer electrolyte membrane fuel cells performance, *Int. J. Hydrogen Energy* 41 (2016) 19771–19780.
- [7] Y. Kawamura, N. Ogura, T. Yamamoto, A. Igarashi, A miniaturized methanol reformer with Si-based microreactor for a small PEMFC, *Chem. Eng. Sci.* 61 (2006) 1092–1101.
- [8] K. Scott, W.M. Taama, P. Argyropoulos, K. Sundmacher, The impact of mass transport and methanol crossover on the direct methanol fuel cell, *J. Power Sources* 83 (1999) 204–216.
- [9] J.S. Wainright, J.T. Wang, D. Weng, R.F. Savinell, M. Litt, Acid-Doped Polybenzimidazoles: a new polymer electrolyte, *J. Electrochem. Soc.* 142 (1995) 121–123.
- [10] X. Zhao, W. Yuan, Q. Wu, H. Sun, Z. Luo, H. Fu, High-temperature passive direct methanol fuel cells operating with concentrated fuels, *J. Power Sources* 273 (2015) 517–521.
- [11] J.T. Wang, R.F. Savinell, J. Wainright, M. Litt, H. Yu, A H-2/O-2 fuel cell using acid doped polybenzimidazole as polymer electrolyte, *Electrochim. Acta* 41 (1996) 193–197.
- [12] J. Kerres, A. Ullrich, F. Meier, T. Haring, Synthesis and characterization of novel acid-base polymer blends for application in membrane fuel cells, *Solid State Ionics* 125 (1999) 243–249.
- [13] D.J. Jones, J. Roziere, Recent advances in the functionalisation of polybenzimidazole and polyetherketone for fuel cell applications, *J. Membr. Sci.* 185 (2001) 41–58.
- [14] Y.L. Ma, J.S. Wainright, M.H. Litt, R.F. Savinell, Conductivity of PBI membranes for high-temperature polymer electrolyte fuel cells, *J. Electrochem. Soc.* 151 (2004) 8–16.
- [15] S.S. Araya, et al., A comprehensive review of PBI-based high temperature PEM fuel cells, *Int. J. Hydrogen Energy* 41 (2016) 21310–21344.
- [16] A. Chandan, et al., High temperature (HT) polymer electrolyte membrane fuel cells (PEMFC) - a review, *J. Power Sources* 231 (2013) 264–278.
- [17] S. Authayanun, K. Im-Orb, A. Arpornwihanop, A review of the development of high temperature proton exchange membrane fuel cells, *Chin. J. Catal.* 36 (2015) 473–483.
- [18] L. Alejo, R. Lago, M.A. Pena, J.L.G. Fierro, Partial oxidation of methanol to produce hydrogen over Cu-Zn-based catalysts, *Appl. Catal. Gen.* 162 (1997) 281–297.
- [19] M.P. Harold, B. Nair, G. Kolios, Hydrogen generation in a Pd membrane fuel processor: assessment of methanol-based reaction systems, *Chem. Eng. Sci.* 58 (2003) 2551–2571.
- [20] J. Agrell, H. Birgersson, M. Boutonnet, I. Melian-Cabrera, R.M. Navarro, J.G. Fierro, Production of hydrogen from methanol over Cu/ZnO catalysts promoted by ZrO<sub>2</sub> and Al<sub>2</sub>O<sub>3</sub>, *J. Catal.* 219 (2003) 389–403.
- [21] C. Cao, K.L. Hohn, Study of reaction intermediates of methanol decomposition and catalytic partial oxidation on Pt/Al<sub>2</sub>O<sub>3</sub>, *Appl. Catal. Gen.* 354 (2009) 26–32.
- [22] S. Schuyten, E.E. Wolf, Selective combinatorial studies on Ce and Zr promoted Cu/Zn/Pd catalysts for hydrogen production via methanol oxidative reforming, *Catal. Lett.* 106 (2006) 7–14.
- [23] Z. Wang, J. Xi, W. Wang, G. Lu, Selective production of hydrogen by partial oxidation of methanol over Cu/Cr catalysts, *J. Mol. Catal. Chem.* 191 (2003) 123–134.
- [24] H.S. Wang, K.Y. Huang, Y.J. Huang, Y.C. Su, F.G. Tseng, A low-temperature partial-oxidation-methanol micro reformer with high fuel conversion rate and hydrogen production yield, *Appl. Energy* 138 (2015) 21–30.
- [25] B. Lindstrom, L.J. Pettersson, Hydrogen generation by steam reforming of methanol over copper-based catalysts for fuel cell applications, *Int. J. Hydrogen Energy* 26 (2001) 923–933.
- [26] T. Takahashi, M. Inoue, T. Kai, Effect of metal composition on hydrogen selectivity in steam reforming of methanol over catalysts prepared from amorphous alloys, *Appl. Catal. Gen.* 218 (2001) 189–195.
- [27] H. Purnama, T. Ressler, R.E. Jentoft, H. Soerijanto, R. Schlogl, R. Schomacker, CO formation/selectivity for steam reforming of methanol with a commercial CuO/ZnO/Al<sub>2</sub>O<sub>3</sub> catalyst, *Appl. Catal. Gen.* 259 (2004) 83–94.
- [28] T. Shishido, et al., Water-gas shift reaction over Cu/ZnO and Cu/ZnO/Al<sub>2</sub>O<sub>3</sub> catalysts prepared by homogeneous precipitation, *Appl. Catal. Gen.* 303 (2006) 62–71.
- [29] Y.F. Han, M. Kinne, R.J. Behm, Selective oxidation of CO on Ru/gamma-Al<sub>2</sub>O<sub>3</sub> in methanol reformat at low temperatures, *Appl. Catal. B Environ.* 52 (2004) 123–134.
- [30] G. Avgouropoulos, T. Ioannides, C. Papadopoulou, J. Batista, S. Hocevar, H.K. Matralis, A comparative study of Pt/gamma-Al<sub>2</sub>O<sub>3</sub>, Au/alpha-Fe<sub>2</sub>O<sub>3</sub> and CuO-CeO<sub>2</sub> catalysts for the selective oxidation of carbon monoxide in excess hydrogen, *Catal. Today* 75 (2002) 157–167.
- [31] A.J. Dyakonov, Abatement of CO from relatively simple and complex mixtures: I. Oxidation on Pd-Ag/zeolite catalysts, *Appl. Catal. B Environ.* 45 (2003) 241–255.
- [32] H. Koga, S. Fukahori, T. Kitaoka, A. Tomoda, R. Suzuki, H. Wariishi, Auto-thermal reforming of methanol using paper-like Cu/ZnO catalyst composites prepared by a papermaking technique, *Appl. Catal. Gen.* 309 (2006) 263–269.
- [33] B. Park, S. Kwon, Compact design of oxidative steam reforming of methanol assisted by blending hydrogen peroxide, *Int. J. Hydrogen Energy* 40 (2015) 12697–12704.
- [34] S. Patel, K.K. Pant, Activity and stability enhancement of copper–alumina catalysts using cerium and zinc promoters for the selective production of hydrogen via steam reforming of methanol, *J. Power Sources* 159 (2006) 139–143.
- [35] S. Liu, K. Takahashi, K. Fuchigami, K. Uematsu, Hydrogen production by oxidative methanol reforming on Pd/ZnO: catalyst deactivation, *Appl. Catal. Gen.* 299 (2006) 58–65.
- [36] S. Schuyten, S. Guerrero, J.T. Miller, T. Shibata, E.E. Wolf, Characterization and oxidation states of Cu and Pd in Pd–CuO/ZnO/ZrO<sub>2</sub> catalysts for hydrogen production by methanol partial oxidation, *Appl. Catal. Gen.* 352 (2009) 133–144.
- [37] F.V. Vázquez, P. Simell, J. Pennanen, J. Lehtonen, Reactor design and catalysts testing for hydrogen production by methanol steam reforming for fuel cells applications, *Int. J. Hydrogen Energy* 41 (2016) 924–935.
- [38] T. Kim, S. Kwon, Integrated fabrication of a micro methanol reformer and a hydrogen peroxide heat source, in: 20th IEEE International Conference on Micro Electro Mechanical Systems (MEMS 2007), 2007, pp. 894–897.

- [39] S. Zhang, Y. Zhang, J. Chen, X. Zhang, X. Liu, High yields of hydrogen production from methanol steam reforming with a cross-U type reactor, *PloS One* 12 (2017).
- [40] R. Chein, Y.C. Chen, J.Y. Chen, J.N. Chung, Design and test of a miniature hydrogen production reactor integrated with heat supply, fuel vaporization, methanol-steam reforming and carbon monoxide removal unit, *Int. J. Hydrogen Energy* 37 (2012) 6562–6571.
- [41] K. Yoshida, S. Tanaka, H. Hiraki, M. Esashi, A micro fuel reformer integrated with a combustor and a microchannel evaporator, *J. Micromech. Microeng.* 16 (2006) 191–197.
- [42] J.D. Holladay, E.O. Jones, R.A. Dagle, G.G. Xia, C. Cao, Y. Wang, High efficiency and low carbon monoxide micro-scale methanol processors, *J. Power Sources* 131 (2004) 69–72.
- [43] G. Wang, P. Cheng, H. Wu, Unstable and stable flow boiling in parallel microchannels and in a single microchannel, *Int. J. Heat Mass Tran.* 50 (2007) 4297–4310.
- [44] F. Weng, C.K. Cheng, K.C. Chen, Hydrogen production of two-stage temperature steam reformer integrated with PBI membrane fuel cells to optimize thermal management, *Int. J. Hydrogen Energy* 38 (2013) 6059–6064.
- [45] G. Avgouropoulos, J. Papavasiliou, M.K. Daletou, J.K. Kallitsis, T. Ioannides, S. Neophytides, Reforming methanol to electricity in a high temperature PEM fuel cell, *Appl. Catal. B Environ.* 90 (2009) 628–632.
- [46] G. Avgouropoulos, S.G. Neophytides, Performance of internal reforming methanol fuel cell under various methanol/water concentrations, *J. Appl. Electrochem.* 42 (2012) 719–726.
- [47] G. Avgouropoulos, A. Paxinou, S. Neophytides, In situ hydrogen utilization in an internal reforming methanol fuel cell, *Int. J. Hydrogen Energy* 39 (2014) 18103–18108.
- [48] G. Avgouropoulos, J. Papavasiliou, T. Ioannides, S. Neophytides, Insights on the effective incorporation of a foam-based methanol reformer in a high temperature polymer electrolyte membrane fuel cell, *J. Power Sources* 296 (2015) 335–343.
- [49] P. Ribeirinha, I. Alves, F.V. Vazquez, G. Schuller, M. Boaventura, A. Mendes, Heat integration of methanol steam reformer with a high-temperature polymeric electrolyte membrane fuel cell, *Energy* 120 (2017) 468–477.
- [50] P. Ribeirinha, G. Schuller, M. Boaventura, A. Mendes, Synergetic integration of a methanol steam reforming cell with a high temperature polymer electrolyte fuel cell, *Int. J. Hydrogen Energy* 42 (2017) 13902–13912.
- [51] H.S. Wang, C.P. Chang, Y.J. Huang, Y.C. Su, F.G. Tseng, A high-yield and ultra-low-temperature methanol reformer integratable with phosphoric acid fuel cell (PAFC), *Energy* 133 (2017) 1142–1152.
- [52] H.S. Wang, K.Y. Huang, Y.J. Huang, Y.C. Su, F.G. Tseng, A low-temperature partial-oxidation-methanol micro reformer with high fuel conversion rate and hydrogen production yield, *Appl. Energy* 138 (2015) 21–30.
- [53] C.L. Lu, C.P. Chang, Y.H. Guo, T.K. Yeh, Y.C. Su, P.C. Wang, F.G. Tseng, High-performance and low-leakage phosphoric acid fuel cell with synergic composite membrane stacking of micro glass microfiber and nano PTFE, *Renew. Energy* 134 (2019) 982–988.
- [54] D. Bogojevic, et al., Experimental investigation of non-uniform heating effect on flow boiling instabilities in a microchannel-based heat sink, *Int. J. Therm. Sci.* 50 (2011) 309–324.
- [55] H.-S. Wang, et al., A high-yield and ultra-low-temperature methanol reformer integratable with phosphoric acid fuel cell (PAFC), *Energy* 133 (2017) 1142–1152.
- [56] G. Schuller, et al., Heat and fuel coupled operation of a high temperature polymer electrolyte fuel cell with a heat exchanger methanol steam reformer, *J. Power Sources* 347 (2017) 47–56.